JOURNAL OF SCIENCE
SAKARYA UNIVERSITY

Sakarya University Journal of Science

ISSN 1301-4048 | e-ISSN 2147-835X | Period Bimonthly | Founded: 1997 | Publisher Sakarya University |
http://www.saujs.sakarya.edu.tr/

Title: Design and Implementation of a Step-Up Power Converter for Renewable Resource Application

Authors: Davood Ghaderi
Recieved: 2018-12-27 16:39:06

Accepted: 2019-10-13 14:07:34

Article Type: Research Article
Volume: 24
Issue: 1
Month: February
Year: 2020
Pages: 86-97

How to cite
Davood Ghaderi; (2020), Design and Implementation of a Step-Up Power Converter for Renewable Resource Application . Sakarya University Journal of Science, 24(1), 86-97, DOI: 10.16984/saufenbilder.503954
Access link
http://www.saujs.sakarya.edu.tr/tr/issue/49430//503954

Sakarya University Journal of Science 24(1), 86-97, 2020

Design and Implementation of a Step-Up Power Converter for Renewable Resource Application

Davood Ghaderi[1]

Abstract

Renewable energy sources including photovoltaic panels, wind turbines and fuel cells widely are spreading. Among all the renewable energy sources, solar power generation system tops the list. The first choice is the boost converter when the voltage step up is the issue. But the most important subject is applying an efficient structure with high gain, cheap and quick controller circuit. Our proposed modified boost converter (MBC) is one of such converter which consists of several cheap components such as diode, inductor, capacitor and power switch, which has same switching frequency and phase shift in comparison with conventional boost converters. The voltage gain of the proposed structure is very high in comparison with conventional boost converter and by forming a preamplifier layer, for a duty cycle of 80% by adding only two diodes, one inductor, and one capacitor, voltage gain is increased by 5 times compared to the classic boost converter. The proposed method provides the increased output voltage along with duty cycle and voltage gain reaches to 10 times in comparison with classic boost structure. The projected strategy has been verified with the help of MATLAB/SIMULINK. Also, a hardware implementation of proposed MBC has been done in a laboratory scale around 100W.

Keywords: DC-DC converter, Renewable energy application, High gain, Boosting structure.

1. INTRODUCTION

Today, renewable energy sources such as solar energy and wind energy have become an alternative energy source as fossil fuels have shortened in a short time and the severe damage to the environment.

However, the disadvantage of solar energy and wind energy is that they are affected by the natural conditions their efficiency changes according to these conditions [1], [13]. Switching mode resources can be used for many purposes, including DC-DC converters. Often, even though a DC source such as a battery is available, that's voltage is not suited to the need of the system.

[1] e-mail: davood.ghaderi@btu.edu.tr, Orcid: 0000-0003-2234-3453, Electrical and Electronics Engineering Department of Bursa Technical University, Bursa, Turkey

For example, motors which are used to drive electric cars require higher voltages than the 500V field supplied with a stand-alone battery. Even if the batteries were used, the extra weight and space needed would be too large to prevent the practicality of the system. The solution is to use less battery and raise the existing voltage to the desired level using an amplifier-converter.

Another problem with large or small batteries is that the output voltage changes when the current charge is depleted and the battery voltage is insufficient to provide power to the given power supply. However, if this low output level can be raised to the nominal level again using a boost converter, battery life can be extended [1-4].

The input to a boost converter can be a DC from a network inverter, as well as from many sources such as solar panels, fuel cells, and DC generators, as well as solid waste batteries. The Boost converter differs from the Buck converter in that the output voltage is equal to or greater than the input voltage.

The main areas where DC-DC boost converters are used are; automotive applications, power amplifier applications, adaptive control applications, battery power systems, consumer electronics and communication applications [5-10].

In order to reduce the component count, single switch quadratic boost converters commonly are integrated.

There are different designing of this structure were proposed in [11-13].

However, the conduction loss and switching loss are increased because the currents of each boost cell flow into only one common switch [14-17].

Hence, soft switching technology and the reduction in switch voltage including zero voltage ZVS and zero current switching ZCS, are required to improve power efficiency.

In [18], zero-voltage-switching (ZVS) operation was implemented to improve power efficiency, but an additional switch is required and the control circuit is complex.

In another method to obtain high voltage gain, a coupled inductor can be used instead of the main inductor.

The high-step-up boost converters using a coupled inductor were proposed in [19-20]. The turn ratio of the coupled inductor is utilized to adjust the voltage gain. However, because a high turn ratio is required to obtain a high voltage gain, the size of the coupled inductor and the conduction loss of the winding increase. Moreover, a snubber circuit or clamping circuit is needed due to the leakage inductance from the coupled inductor [19-20].

This clamping circuit not only reduces the switch voltage stress but also provides ZVS operation. In [17], the passive/active snubbers were proposed by using additional inductors, capacitors, and diodes with the active switch.

Flyback boost converter also has suggested but it has more losses in comparison with classic and quadratic boost converters because of using transformers [21].

Our study is introducing a simple and cheap modified boost converter without any extra power switch with the ability to provide efficient and high voltage gain. In comparison with the classic boost converter, projected converter providing a 10 times greater as voltage gain approximately at the same efficiency.

The proposed circuit is preparing a preamplifier block between the input inductor and semiconductor switch and acts as a cascaded structure.

2. MODİFİED BOOST CONVERTER

2.1. Small signal analysis of structure in switch on and off modes

Figure 1a and 1b show a conventional and our proposed boost converters respectively. As can be seen, a boosting structure is located between the entrance inductor and the power switch.

Based on switch on or off working modes, only one of the D_1 and D_2 diodes will be active in structure and by this way, it makes a preamplifier layer for boosting purposes. All small signal and mathematical analysis have stipulated for both states.

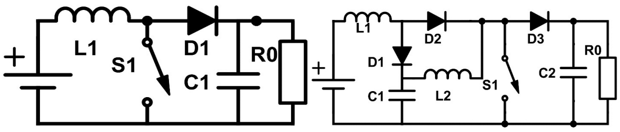

(a) (b)

Figure 1 (a) Conventional and (b) Modified Boost structures

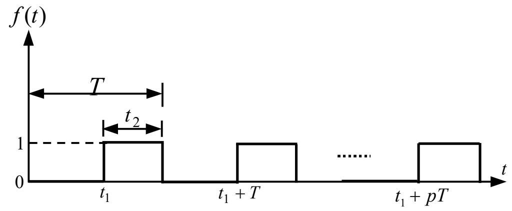

Figure 2 Pulse Width Modulation (PWM) which is applied to the power switch. Per period (T) contains of two $(0,t_1)$ and (t_1,T) intervals

Figure 2 presents the PWM wave applying to the power switch in the boost converter. In this figure for $[0,t_1]$ and [t1, T] time intervals respectively Switch S_1, is off and on. So, if we consider $[t_1, T]$ interval as DT, the $[0, t_1]$ interval will be (1-D) T. In another word, D is the duty cycle of power switch S_1.

Mode 1: For a time interval that power switch receives the pulse and is the short circuit, both L_1 and L_2 are magnetizing. This issue will be done by input voltage through diode D_2 and the power switch for L_1 and from C_1 and switch for L_2.

As can be seen in this mode, D_1 is in off mode. Based on this statement currents of inductors are rising in the on state. As predicted the voltage value on capacitor C1 is discharging on L2 through the power switch and decreases.

Also, the voltage on output capacitor is discharging on output load in this mode. The current value of diode D_1 is zero and because of conducting od diode D_2, its current will increases.

Figure 3a shows the on state of the power switch in projected structure and figure 3b illustrates the simplified form of figure 3a.

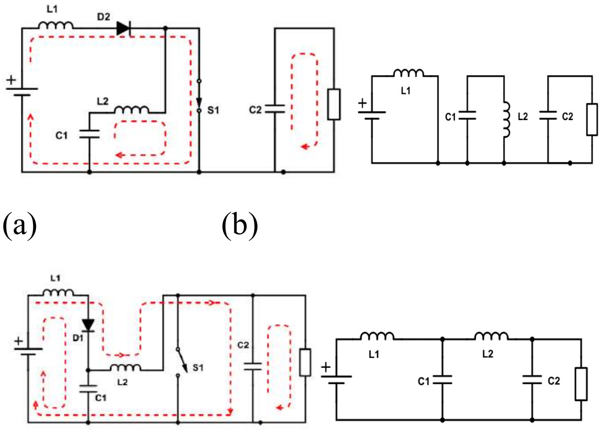

(a) (b)

(c) (d)

Fig. 3. State of proposed structure (a) when the power switch is on and (b) simplified form of the converter in on mode, (c) when the power switch is off and (d) simple view in off mode

Based on these situations the current waveform passes through inductor L_1 can be written as below:

$$L_1 \frac{di_{L1}}{dt} = V_{in} \Rightarrow \frac{di_{L1}}{dt} = \frac{V_{in}}{L_1} \quad (1)$$

Also current of inductor L_2 is:

$$L_2 \frac{di_{L2}}{dt} = v_{C1} \Rightarrow \frac{di_{L2}}{dt} = \frac{v_{C1}}{L_2} \tag{2}$$

Voltage waveform for capacitor C_1 can be gained as:

$$C_1 \frac{dv_{C1}}{dt} = -i_{L2} \Rightarrow \frac{dv_{C1}}{dt} = -\frac{i_{L2}}{C_1} \tag{3}$$

And finally we can find the voltage for the output capacitor as equation 4:

$$C_2 \frac{dv_o}{dt} = -\frac{v_o}{R} \Rightarrow \frac{dv_o}{dt} = -\frac{v_o}{C_2 R} \tag{4}$$

So, the steady state matrix of no interval will be equal with equation (5):

$$\begin{bmatrix} \dot{i}_{l1} \\ \dot{i}_{l2} \\ \dot{v}_{c1} \\ \dot{v}_{c2} \end{bmatrix} = \begin{bmatrix} 0 & 0 & 0 & 0 \\ 0 & 0 & \frac{1}{L_2} & 0 \\ 0 & -\frac{1}{C_1} & 0 & 0 \\ 0 & 0 & 0 & -\frac{1}{RC_2} \end{bmatrix} \begin{bmatrix} i_{l1} \\ i_{l2} \\ v_{c1} \\ v_{c2} \end{bmatrix} + \begin{bmatrix} \frac{1}{L_1} \\ 0 \\ 0 \\ 0 \end{bmatrix} [V_{in}] \tag{5}$$

Mode 2: Figure 3c and 3d illustrate the state of the circuit when power MOSFET is off and its simplified view.

In this time interval, L_1 is demagnetizing on capacitor C_1 through D_1 and D_2 is in off mode. Also, inductor L_2 is demagnetizing through the D_3 diode on output capacitor and load.

In this time interval, as mentioned the voltage values on capacitors C_1 and C_2 will increases through L_1 and L_2 respectively.

Figure 4 illustrates all components conductions in both on and off modes of power MOSFET.

Small signal analysis for this state also has been analyzed and written below. For inductor L_1 we can calculate:

$$\begin{aligned} & L_1 \frac{di_{L1}}{dt} = (V_{in} - v_{C1})(1-d) \\ & \Rightarrow \frac{di_{L1}}{dt} = \frac{V_{in} - v_{C1}}{L_1}(1-d) \end{aligned} \tag{6}$$

Also, the current waveform of inductor L_2 is equal with:

$$\begin{aligned} & L_2 \frac{di_{L2}}{dt} = (v_{C1} - v_o)(1-d) \\ & \Rightarrow \frac{di_{L2}}{dt} = \frac{v_{C1} - v_o}{L_2}(1-d) \end{aligned} \tag{7}$$

Voltage waveform for capacitor C_1:

$$\begin{aligned} & C_1 \frac{dv_{C1}}{dt} = (i_{L1} - i_{L2})(1-d) \\ & \Rightarrow \frac{dv_{C1}}{dt} = \frac{i_{L1} - i_{L2}}{C_1}(1-d) \end{aligned} \tag{8}$$

And for C_2:

$$\begin{aligned} & C_2 \frac{dv_o}{dt} = (i_{L2} - \frac{v_o}{R})(1-d) \\ & \Rightarrow \frac{dv_o}{dt} = \frac{i_{L2} - \frac{v_o}{R}}{C_2}(1-d) \end{aligned} \tag{9}$$

For this time interval, steady state matrix will be:

$$\begin{bmatrix} \dot{i}_{l1} \\ \dot{i}_{l2} \\ \dot{v}_{c1} \\ \dot{v}_{c2} \end{bmatrix} = \begin{bmatrix} 0 & 0 & -\frac{1}{L_1} & 0 \\ 0 & 0 & \frac{1}{L_2} & -\frac{1}{L_2} \\ \frac{1}{C_1} & -\frac{1}{C_1} & 0 & 0 \\ 0 & \frac{1}{C_2} & 0 & -\frac{1}{RC_2} \end{bmatrix} \begin{bmatrix} i_{l1} \\ i_{l2} \\ v_{c1} \\ v_{c2} \end{bmatrix} + \begin{bmatrix} \frac{1}{L_1} \\ 0 \\ 0 \\ 0 \end{bmatrix} [V_{in}] \tag{10}$$

So according to an on and off intervals of a PWM for proposed structure current and voltage waveforms for inductors L_1 and L_2 and capacitors C_1 and C_2 can be proposed as below equations:

$$\frac{di_{L1}}{dt} = -\frac{(1-d)}{L_1} v_{C1} + \frac{1}{L_1} V_{in} \tag{11}$$

$$\frac{di_{L2}}{dt} = \frac{1}{L_2} v_{C1} - \frac{(1-d)}{L_2} v_o \quad (12)$$

$$\frac{dv_{C1}}{dt} = \frac{(1-d)}{C_1} i_{L1} - \frac{1}{C_1} i_{L2} \quad (13)$$

$$\frac{dv_o}{dt} = \frac{(1-d)}{C_2} i_{L2} - \frac{1}{RC_2} v_o \quad (14)$$

The steady state matrix of this structure by using equations 1 to 14 can be written as below:

$$\begin{bmatrix} \dot{i}_{l1} \\ \dot{i}_{l2} \\ \dot{v}_{c1} \\ \dot{v}_{c2} \end{bmatrix} = \begin{bmatrix} 0 & 0 & -\frac{1-d}{L_1} & 0 \\ 0 & 0 & \frac{1}{L_2} & -\frac{1-d}{L_2} \\ \frac{1-d}{C_1} & -\frac{1}{C_1} & 0 & 0 \\ 0 & \frac{1-d}{C_2} & 0 & -\frac{1}{RC_2} \end{bmatrix} \begin{bmatrix} i_{l1} \\ i_{l2} \\ v_{c1} \\ v_{c2} \end{bmatrix} + \begin{bmatrix} \frac{1}{L_1} \\ 0 \\ 0 \\ 0 \end{bmatrix} [V_{in}]$$

(15)

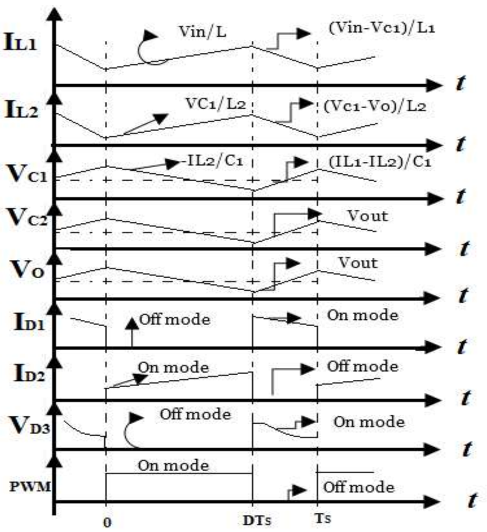

Figure 4 Mode of operation of the proposed structur

2.2. Voltage gain analysis of proposed modified boost converter

By considering the internal resistance of inductors, figure 5 illustrates an approximate model of the proposed converter. In this model, it has been assumed that all inductors with internal resistance and power semiconductors including diodes and power switch have a Vx value as voltage drop. This value has been considered as a Vx value for all components for more simplicity and reducing the analysis complexity. Based on charging and discharging states of inductors, mathematical evaluation for the voltage gain will appear in two different modes.

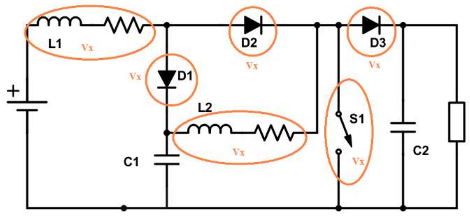

Figure 5 The equivalent circuit for the proposed converter by considering the internal resistances and components voltage drop

State 1: voltage across inductor L_1 when the power switch is in on and off modes:

When power semiconductor switch is in on mode, the voltage across inductor L_1 will be equal with:

$$\begin{aligned} &(V_{in} - 3V_x)D + (V_{in} - V_{C1} - 2V_x)(1-D) = 0 \\ &\Rightarrow V_{c1} = V_{in}\left(\frac{1}{1-D}\right) - V_x\left(\frac{2+D}{1-D}\right) \end{aligned} \quad (16)$$

In the above equation, D is for a time interval that the switch is in on mode and (1-D) is for the off state of MOSFET. Also, the voltage drop on inductor L_2 for the switch on and off intervals can be calculated as equation (17):

$$\begin{aligned} &(V_{c1} - 2V_x)D + (V_{c1} - V_o - 2V_x)(1-D) = 0 \\ &\Rightarrow V_o = V_{c1}\left(\frac{1}{1-D}\right) - V_x\left(\frac{2}{1-D}\right) \end{aligned} \quad (17)$$

By replacing the equation (16) into equation (17), the voltage gain of the proposed structure can be calculated:

$$V_o = \frac{V_{in}(\frac{1}{1-D}) - V_x(\frac{2+D}{1-D})}{1-D} - 2V_x(\frac{1}{1-D})$$
$$\Rightarrow V_o = \frac{V_{in} - V_x(4-D)}{(1-D)^2} - 2V_X(\frac{1}{1-D}) \tag{18}$$
$$\Rightarrow V_o = V_{in}\frac{1}{(1-D)^2} - V_X(\frac{4-D}{(1-D)^2})$$

As an approximate response for equation (18), by neglecting of Vx in a simple and close to real state, the output voltage and voltage gain can be written as equations (19) and (20).

$$V_o = V_{in}\frac{1}{(1-D)^2} \tag{19}$$

$$G = \frac{V_o}{V_{in}} = \frac{1}{(1-D)^2} \tag{20}$$

And by a simple calculation the relation between input and output current values can be calculated as:

$$I_o = I_{in}(1-D)^2 \tag{21}$$

2.3. The design stages of the control circuit

Thy key point for controller designing is finding an equation between the output voltage and one of inductors currents or capacitor voltages derivatives and it can be obtained from equation (9):

$$C_2\frac{dv_o}{dt} + \frac{1}{R}v_o = (1-d)i_{L_2} = u \tag{22}$$

u is the PI controller output signal and d is the duty cycle of PWM which will be implemented to power MOSFET. Equation (22) can be rewritten in a simpler way as:

$$d = 1 - \frac{u}{i_{L_2}} \tag{23}$$

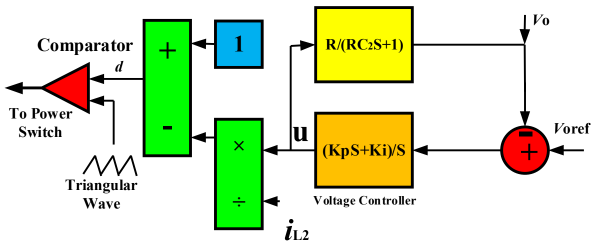

Figure 6 Voltage comparison, PI control and PWM modulator blocks

The general form of a PI controller comes from:

$$G(s) = k_p + \frac{k_i}{s} = \frac{k_p s + k_i}{s} \tag{24}$$

We can put equation (22) in a feedback loop by a PI controller as Figure 7.

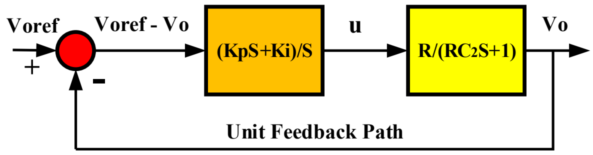

Figure 7 Closed loop form of the PI controlled cascade boost structure

The transfer function of closed loop form of this feedback is equal with:

$$G_F = \frac{G_o}{1+G_o} = \frac{\frac{1}{C_2}(k_p + k_i)}{s^2 + (\frac{1+Rk_p}{RC_2}) + \frac{k_i}{C_2}} \tag{25}$$
$$\Rightarrow G_F = \frac{\frac{1}{C_2}(k_p s + k_i)}{s^2 + 2\xi\omega_0 s + \omega_o^2}$$

It is easy to gain:

$$\begin{cases} \dfrac{1+Rk_p}{RC_2} = 2\xi\omega_0 \\ \dfrac{k_i}{C_2} = \omega_0^2 \end{cases} \Rightarrow \begin{cases} k_p = 2\xi\omega_0 C_2 - \dfrac{1}{R} \\ k_i = \omega_0^2 C_2 \end{cases} \quad (26)$$

The better value for damping factor ξ is 0.707. Since ω_0 is a pulsation, chosen less than switching frequency ω_s to get the best response. Fırst Page Requırements

3. SIMULATION RESULTS

A group of simulation has been done in Matlab Simulink R2017a for evaluation and test of the stability of the proposed circuit.

The input voltage for the structure has been fixed in 24VDC and output load value has been chosen as 100 ohms. Also, 50KHz as switching frequency has been considered.

Simulation has done for duty cycle from 30% to 90% and results have shown in figures 9,10 and 11.

Table 1 presents all components and parameters which have been used in the simulation. For our tests, we assumed the internal resistance for both inductors, 0.1 ohms for inductor L_1 and 0.05 ohm for inductor L_2. Figure 8a illustrates the final diagram of proposed converter and controller and as it can show a sampling has been done based on equation (9) for controller designing.

This diagram is suitable for all kind of renewable energy sources since producing limited values of power because of the high efficiency of the projected circuit and it has been reported in figure 9.

Also, figure 8b shows the implemented prototype. Figure 9 shows the efficiency diagram and has been done a comparison between conventional and projected prototypes.

The most important subject that can be a reason of high efficiency for the new converter is its components especially power diodes.

As mentioned in section 2.1, in any time interval of PWM, only one diode will be located in the current direction and will charge the inductors or output capacitor.

Table 1. Particularization of the projected boost converter

Parameter	Value (unit)
power	100 W
Input voltage	24 VDC
L_1	200 uH
R_1 (internal resistance of L_1)	0.1 ohm
L_2	100 uH
R_2 (internal resistance of L_2)	0.05 ohm
C_1	56 uF
C_2	47 uF
Duty cycle	30 % - 90 %
Switching frequency	50 KHz

Figure 10 shows the voltage gain for proposed and conventional boost circuits. Also expected and ideal values for different duty cycles have been reported in this figure.

One of the most important issues for a boost converter is the converter's ability in gain production since voltage transfer is preferred rather than the current transition in all parts of fossil or renewable energy sources.

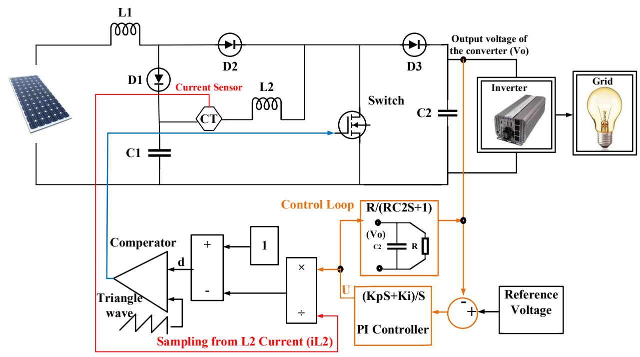

(a)

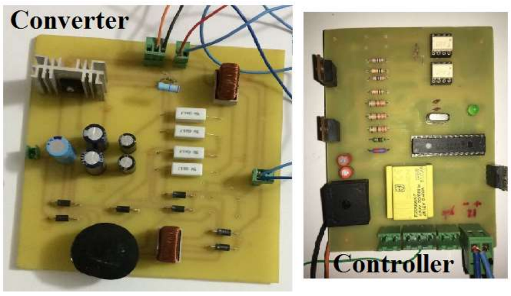

(b)

Figure 8 proposed structure with designed controller block (a) in simulation and (b) implementation

Figure 11 illustrates the controller performance and stability in producing of different voltages in output. For this simulation, the input supply has been fixed to 12VDC and the reference voltage is changing between 80, 100 and 120VDC.

For our tests in order to PWM implementation to gate-source pins of power semiconductor switch, the triangle waveform has been considered with 50KHz frequency.

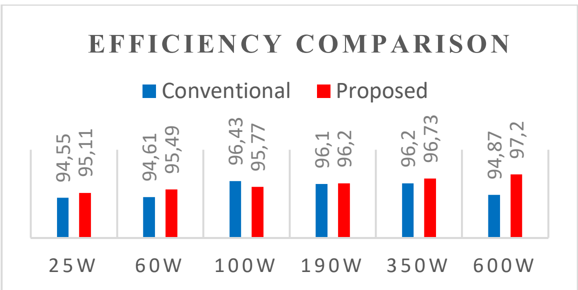

Figure 9 Efficiency diagram for proposed and conventional structures

Figure 11 shows the controller performance in the tracking of desired voltage values in structure's output and by changing to different voltages it can track and reach to these voltages only in less than 10 ms without any undershoot or overshoot in signals.

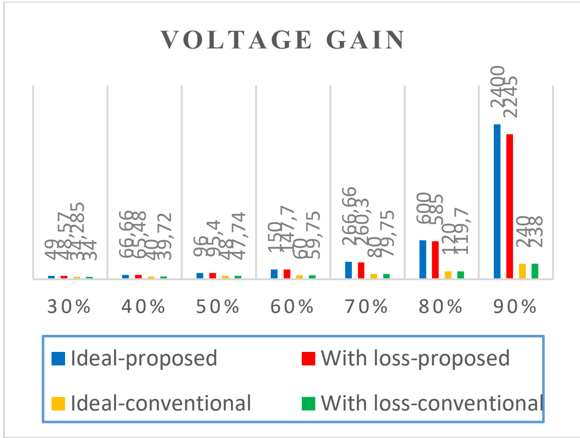

Figure 10 Voltage gain diagram for proposed and conventional structures in real and ideal states based on different duty cycles

For a duty cycle of 50%, the projected circuit can produce two times more than conventional structure and this ratio is greater in the higher amount of duty cycles and in 80% and 90% this ratio receives to five and ten times respectively.

It means with applying of the proposed converter will expect to receive to 2400VDC in structure's output by 24VDC in input since a conventional boost converter only can give 240VDC though in the simulation we received to 2245VDC and is a good result by considering of different structures results.

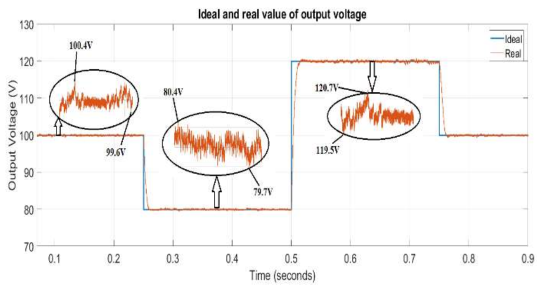

Figure 11 Tracking and output voltage of the proposed structure

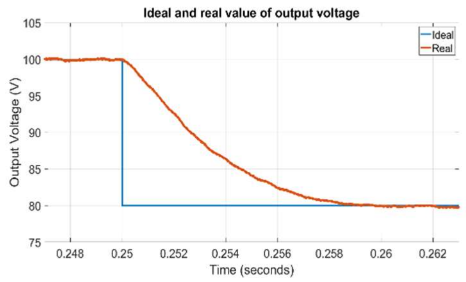

(a)

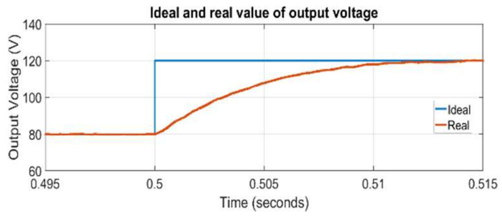

(b)

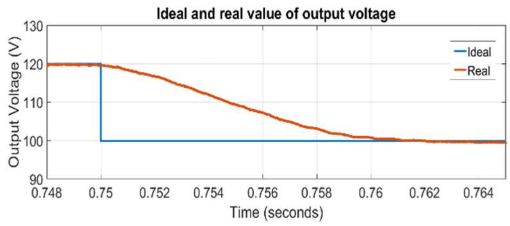

(c)

Figure 12 Time delay diagrams for tracking of the desired voltage in the proposed converter's output when a change (a) from 100VDC to 80VDC, (b) from 80VDC to 120VDC and (c) from 120VDC to 100VDC

4. EXPERIMENTAL RESULTS

A prototype with 100W has been implemented and figure 12,13 and 14 show the results. Input voltage and switching frequency have been fixed in 4VDC and 50KHz respectively. Inductor L_1 has been fixed to 200uH and L_2 to 100uH. Also, capacitor C_1 value has been considered as 68uF and output capacitor C_2 as 470uF. Figure 12 shows the gate source and drain source pulses of structure in 50 and 80 duty cycles and as we expected for different values of on and off intervals of power MOSFET, different voltages for drain-source pins have been obtained. Also, figure 13 illustrates the output voltage and gate-source voltages simultaneously. A fixed DC voltage has been gained in output. Figure 14 shows the oscillation of output voltage in 50% of the duty cycle.

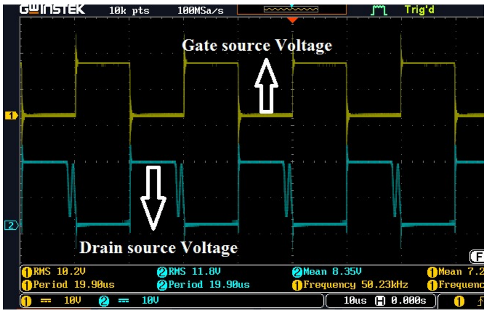

(a)

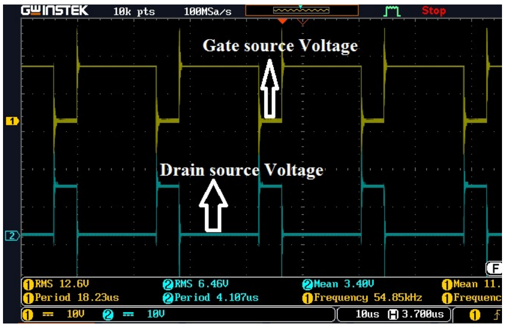

(b)

Figure 12 Gate source and drain-source voltages of the projected structure when the duty cycle is (a) 50% and (b) 80%

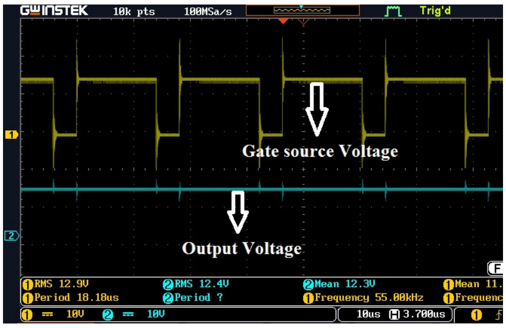

Figure 13 Proposed structure’s ability in boosting the input supply value

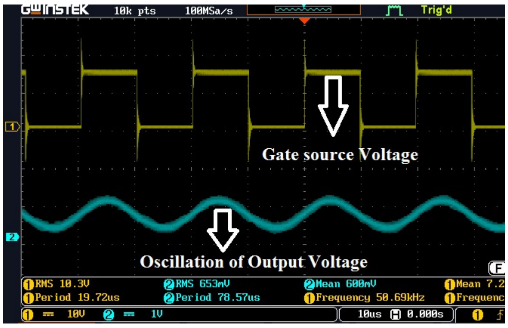

Figure 14 Oscillation domain of output DC voltage in the duty cycle of 50% and switching frequency of 50KHz

5. CONCLUSION

In this study, a high gain DC-DC converter has been investigated. This structure uses a conventional boost converter plus several cheap components including two power diodes, a capacitor, and an inductor. In any time interval of PWM, the circuit current will pass through an only one of diodes, so the efficiency of the projected structure is not impressed. This simple and cheap connection give a preamplifier specification to structure, so converter can give a very high gain compared with a conventional converter. Mathematical analysis and simulation show projected structure by 10VDC as input voltage can give 1000VDC in output by 90% of duty cycle since it is very important for renewable energy sources where these sources produce a very limited amount of power. The efficiency of the structure is comparable with a conventional boost converter by considering new components switching, dynamic, and frequency losses. Also, the controller is designed based on inductors L_2 current sampling and is performing and tracking the desired value of voltage in converter's output in a very limited time interval.

Some advantages of the structure including using only one power semiconductor switch and so no need for extra and complicated controller structure, simple and cheap components and ability to work in a wide range of frequencies. A group of simulation done in Matlab/Simulink 2017a and results confirmed the theoretical and mathematical analysis. A laboratory scaled prototype has been implemented and verifying all mathematical and simulation results. Working in lower switching frequencies will help to decrease voltage and current stresses on power switches where a high gain application is necessary. As a suggestion soft switching and snubber sub-structures can be utilizable for decreasing these stresses.

REFERENCES

[1] M. Lakshmi and S. Hemamalini, "Nonisolated high gain DC-DC converter for DC microgrids," IEEE Trans. Ind. Electron, vol.65, no.2, pp.1205–1212, Feb. 2018.

[2] Shellas Sathyan, Hiralal Murlidhar Suryawanshi, Bhim Singh, Chandan Chakraborty, Vishal Verma, and Maharand Sudhakar Ballal, "Zvs-zcs high voltage gain integrated boost converter for dc microgrid," IEEE Trans. Ind. Electron, vol.63, no.11, pp.6898–6908, Nov. 2016.

[3] Muhammad, Musbahu, Matthew Armstrong, and Mohammed Elgendy, "A nonisolated interleaved boost converter for high-voltage gain applications," IEEE Journal of Emerging and Selected Topics in Power Electronics, vol.4, no.2 pp. 352-362, 2016.

[4] Saadat, Peyman, and Karim Abbaszadeh, "A Single-Switch High Step-Up DC-DC Converter Based on Quadratic Boost," IEEE Transactions on Industrial Electronics, vol.63, no.12, pp.7733-7742, 2016.

[5] Michele Tedesco, Andrea Cipollina, Alessandro Tamburini, and Giorgio Micale, "Towards 1 kW power production in a reverse electrodialysis pilot plant with saline waters and concentrated brines," Journal of Membrane Sci, vol. 522, pp. 226–236, Jan. 2017.

[6] Binwu Wu, Shouxiang Li, Yao Liu, and Keyune Ma Smedley, “A new hybrid boosting converter for renewable energy applications,” IEEE Trans. Power Electron, vol.31, no. 2, pp.1203–1215, Feb. 2016.

[7] Guilherme HF Fuzato, Cassius R. Aguiar, Klebber de A. Ottoboni, Renan F. Bastos, and Ricardo Q. Machado, “Voltage gain analysis of the interleaved boost with voltage multiplier converter used as electronic interface for fuel cells systems,” IET Power Electronics, vol.9, no.9, pp.1842-1851, 2016.

[8] Nagi Yin Yip, David A. Vermaas, Kitty Nijmeijer, and Menachem Elimelech, “Thermodynamic, energy efficiency, and power density analysis of reverse electrodialysis power generation with natural salinity gradients,” Environ. Sci. & Technol, vol.48, no.9, pp.4925–4936, Apr. 2014.

[9] Michele Tedesco, Claudio Scalici, Davide Vaccari, Andrea Cipollina, Alessandro Tamburini, and Giorgio Micale, “Performance of the first reverse electrodialysis pilot plant for power production from saline waters and concentrated brines,” Journal of Membrane Sci, vol.500, pp.33–45, Feb. 2016.

[10] Ying Mei and Chuyang Y. Tang, “Co-locating reverse electro dialysis with reverse osmosis desalination synergies and implications,” Journal of Membrane Sci, vol.539, pp.305-312, 2017.

[11] Mojtaba Forouzesh, Keyvan Yari, Alfred Baghramian, and Sara Hasanpour, “Single switch high step-up converter based on coupled inductor and switched capacitor techniques with quasi-resonant operation,” IET Power Electronics, vol.10, no.2, pp.240–250, 2017.

[12] Giorgio Spiazzi, Davide Biadene, Stefano Marconi, and Andrea Bevilacqua, “Non-isolated high step-up dc-dc converter with minimum switch voltage stress,” Southern Power Electronic Conference (SPEC 2017), Spain, December 2017.

[13] Wei Gao, Yang Zhang, Xing-yu Lv, and Quan-ming Lou, “Non-isolated high-stepup soft switching dc/dc converter with low-voltage stress,” IET Power Electronics, vol. 10, no. 1, pp. 120–128, 2017.

[14] ABdulkasim Bakeer, Mohamed A. Ismeil, Mohamed Orabi, “A powerful finite control set-model predictive control algorithm for quasi Z-source inverter,” IEEE Trans. Ind. Informat, vol.12, no.4, pp.1371-1379, Aug. 2016.

[15] Baoming Ge, Yushan Lu, Hitham Abu-Reb, Robert S. Balog, Fang Zheng Peng, Stephen McMonnell and Xiao Li, “Current ripple damping control to minimize impedance network for single phase quasi-z source system,” IEEE Trans. Ind. Informat, vol.12, no.3, pp.1054-4848, June. 2016.

[16] Minh-Khai Nguyen, Tuan-Vu Le, Sung-Jun Park and Young- cheol Lim, “A class of quasi-switched Boost inverters,” IEEE Trans. Ind. Electron, vol.62, no.3, pp.1526-1536, Mar. 2015.

[17] Anh-Vu Ho, Si-Gyong Yang, Tae-Wou Chun, and Hong-Hee Lee, “Topology of modified switched-capacitor Z-source inverters with improved boost capability,” in Proc. IEEE APEC, 2017, Tampa, Florida, March 2017.

[18] Jie Yang, Dongsheng Yu, He Cheng, Xiaoshu Zan, Huiqing Wen, “Dual-coupled inductors-based high step-up DC/DC converter without input electrolytic capacitor for PV application,” IET Power Electron, vol.10, no.6, pp.646-656, May. 2017.

[19] Minh-Khai Nguyen, Young-Cheol Lim, Joon-Ho Choi and Youn-Ok Choi, “Trans-switched boost inverters,” IET Power

Electron, vol.9, no.5, pp.1065–1073, Apr. 2016.

[20] Yu Tang, Ting Wang, and Yaohua He, “A switched-capacitor-based active network conveter with high voltage gain,” IEEE Trans. on Power Electron, vol.29, no.6, pp.2959–2968, Jun. 2014.

[21] Shelas Sathyan, Hiralal M. Suryawanshi, Amardeep B. Shitole, and Girish G. Talapur, “Soft switched high voltage gain boost integrated flyback converter,” in Proc. 2016 IEEE Int. Conf. Power Electron., Drives Energy Syst., Trivandrum, IN, December 2016.